

## A APPENDIX

### A.1 PROOF OF THEOREM 1

In order to prove our result, we introduce some additional notation. For any probability measure  $\mu \in \mathcal{P}(\mathbb{R})$ , the *support* of the measure  $\mu$  is

$$\text{supp}(\mu) := \{X \in \mathbb{R} : \text{if } X \in N_X \text{ open} \implies \mathcal{P}(N_X) > 0\}. \quad (4)$$

Furthermore, for any set  $A \subseteq \mathbb{R}$ , we use  $\mathbf{1}_A(x) = 1$  if  $x \in A$  and 0 otherwise to denote the characteristic function of the set  $A$ . Furthermore, we use  $\llbracket \cdot \rrbracket$  to denote the Iverson bracket of an event:  $\llbracket A \rrbracket = 1$  if  $A$  is true and 0 otherwise. We will require the use of a Lemma that will aid us in the main proof

**Lemma 1** *For any measure  $\mu \in \mathcal{P}([0, 1])$  with finite support:  $|\text{supp}(\mu)| < \infty$ , let  $\hat{\mu}_n = \frac{1}{n} \sum_{i=1}^n \delta_{x_i}$  where  $x_i \sim \mu$  i.i.d, then we have*

$$|\mu(x) - \hat{\mu}_n(x)| \leq \sqrt{\frac{1}{2n} \log\left(\frac{2}{\delta}\right)}, \quad (5)$$

for a fixed  $x \in \mathbb{R}$  with probability  $1 - \delta$ .

**Proof** Note that  $\mu(x) = \mathbb{E}[\hat{\mu}_n(x)]$  and  $\hat{\mu}_n(x) \in [0, 1]$ . Thus by a standard concentration inequality such as Hoeffding's inequality, we get

$$\mathbb{P}[\llbracket \hat{\mu}_n(x) - \mu(x) \geq t \rrbracket] \leq 2 \exp(-2nt^2). \quad (6)$$

Setting  $t = \sqrt{\frac{1}{2n} \log(2/\delta)}$  completes the proof.  $\blacksquare$

**Lemma 2** *For any measure  $\mu \in \mathcal{P}([0, 1])$  with finite support:  $|\text{supp}(\mu)| < \infty$ , let  $\hat{\mu}_n = \frac{1}{n} \sum_{i=1}^n \delta_{x_i}$  where  $x_i \sim \mu$  i.i.d, then we have*

$$W_1(\mu, \hat{\mu}_n) \leq \sqrt{\frac{|\text{supp}(\mu)|^2}{2n} \log\left(\frac{2 \cdot |\text{supp}(\mu)|}{\delta}\right)}, \quad (7)$$

with probability at least  $1 - \delta$ .

**Proof** We first invoke the Kantorovich-Rubenstein dual of the Wasserstein distance (Villani et al., 2009):

$$W_1(\mu, \hat{\mu}_n) = \sup_{h: [0,1] \rightarrow \mathbb{R}: |h(x) - h(x')| \leq |x - x'|} (\mathbb{E}_\mu[h] - \mathbb{E}_{\hat{\mu}_n}[h]) \quad (8)$$

$$\stackrel{(1)}{\leq} \sup_{h: [0,1] \rightarrow \mathbb{R}: |h(x)| \leq 1} (\mathbb{E}_\mu[h] - \mathbb{E}_{\hat{\mu}_n}[h]) \quad (9)$$

$$\stackrel{(2)}{=} \sup_{A \subseteq [0,1]} (\mathbb{E}_\mu[\mathbf{1}_A] - \mathbb{E}_{\hat{\mu}_n}[\mathbf{1}_A]) \quad (10)$$

$$\stackrel{(3)}{=} \sup_{A \subseteq [0,1]} \left( \sum_{x \in \text{supp}(\mu)} [\mu(x) \cdot \mathbf{1}_A(x)] - \sum_{x \in \text{supp}(\mu)} [\hat{\mu}_n(x) \cdot \mathbf{1}_A(x)] \right) \quad (11)$$

$$= \sup_{A \subseteq [0,1]} \left( \sum_{x \in \text{supp}(\mu)} [\mu(x) - \hat{\mu}_n(x)] \cdot \mathbf{1}_A(x) \right), \quad (12)$$

where (1) is due to fact that  $|x - x'| \leq 1$  for  $x, x' \in [0, 1]$ , (2) is by dual formulation of the Total Variation, and (3) is by the fact that  $\hat{\mu}_n$  is support on  $\text{supp}(\mu)$  by construction. Consider then the following boolean variable

$$H_x = \llbracket |\mu(x) - \hat{\mu}_n(x)| > \sqrt{\frac{1}{2n} \log\left(\frac{2 \cdot |\text{supp}(\mu)|}{\delta}\right)} \rrbracket, \quad (13)$$

we then have by Union bound inequality of probability:

$$\mathbb{P} \left[ \bigcup_{x \in \text{supp}(\mu)} \mathbf{H}_x \right] \leq \sum_{x \in \text{supp}(\mu)} \mathbb{P}[\mathbf{H}_x] \quad (14)$$

$$\leq \sum_{x \in \text{supp}(\mu)} \frac{\delta}{|\text{supp}(\mu)|} \quad (15)$$

$$= \delta. \quad (16)$$

Therefore, we have

$$\mathbb{P} \left[ W_1(\mu, \hat{\mu}_n) \geq \sqrt{\frac{|\text{supp}(\mu)|^2}{2n} \log \left( \frac{2 \cdot |\text{supp}(\mu)|}{\delta} \right)} \right] \quad (17)$$

$$\geq \mathbb{P} \left[ \sup_{A \subseteq [0,1]} \left( \sum_{x \in \text{supp}(\mu)} [\mu(x) - \hat{\mu}_n(x)] \cdot \mathbf{1}_A(x) \right) \geq \sqrt{\frac{|\text{supp}(\mu)|^2}{2n} \log \left( \frac{2 \cdot |\text{supp}(\mu)|}{\delta} \right)} \right] \quad (18)$$

$$\stackrel{(1)}{\geq} \mathbb{P} \left[ \bigcup_{x \in \text{supp}(\mu)} \mathbf{H}_x \right] \quad (19)$$

$$\geq \delta, \quad (20)$$

where (1) is due to the union bound argument, completing the proof.  $\blacksquare$

We are now ready to complete the proof:

$$W_1(\mathcal{P}(\{\hat{\mathbf{r}}^{t_1}\}), \mathcal{P}(\{\hat{\mathbf{r}}^{t_2}\})) \leq W_1(\mathcal{P}(\{\hat{\mathbf{r}}^{t_1}\}), \mathcal{P}(\{\mathbf{r}^{t_1}\})) + W_1(\mathcal{P}(\{\mathbf{r}^{t_1}\}), \mathcal{P}(\{\hat{\mathbf{r}}^{t_2}\})) \quad (21)$$

$$\leq W_1(\mathcal{P}(\{\hat{\mathbf{r}}^{t_1}\}), \mathcal{P}(\{\mathbf{r}^{t_1}\})) \quad (22)$$

$$+ W_1(\mathcal{P}(\{\hat{\mathbf{r}}^{t_2}\}), \mathcal{P}(\{\mathbf{r}^{t_2}\})) + W_1(\mathcal{P}(\{\mathbf{r}^{t_1}\}), \mathcal{P}(\{\mathbf{r}^{t_2}\})) \quad (23)$$

$$\leq 4 \sqrt{\frac{|\text{supp}(\mu)|^2}{2n} \log \left( \frac{2 \cdot |\text{supp}(\mu)|}{\delta} \right)} + W_1(\mathcal{P}(\{\mathbf{r}^{t_1}\}), \mathcal{P}(\{\mathbf{r}^{t_2}\})). \quad (24)$$

Similarly, we can apply the above argument to get

$$W_1(\mathcal{P}(\{\mathbf{r}^{t_1}\}), \mathcal{P}(\{\mathbf{r}^{t_2}\})) \leq 4 \sqrt{\frac{|\text{supp}(\mu)|^2}{2n} \log \left( \frac{2 \cdot |\text{supp}(\mu)|}{\delta} \right)} + W_1(\mathcal{P}(\{\hat{\mathbf{r}}^{t_1}\}), \mathcal{P}(\{\hat{\mathbf{r}}^{t_2}\})). \quad (25)$$

Merging these two together allows us to complete the proof.

## A.2 EVALUATION ON HYPERNERF VRIG DATASET

The HyperNeRF dataset, initially introduced by Park et al. (2021a) and Park et al. (2021b), underwent revisions after Gao et al. (2022) identified certain limitations. These limitations included frames that transitioned abruptly between multiple camera viewpoints in consecutive time steps, a scenario challenging to capture from a single camera, as well as scenes portraying quasi-static scenarios that do not accurately represent real-world dynamics. In response, Gao et al. (2022) proposed an enhanced and more demanding version of this dataset, which we employ for our evaluation. This augmented dataset comprises seven sequences in total, each enriched with keypoint annotations. It encompasses 7 multi-camera captures and 7 single-camera captures, all featuring 480p resolution videos. It is noteworthy that all dynamic scenes within this dataset are inward-facing. For our evaluation, we apply masked metrics as introduced in Gao et al. (2022), which utilize covisibility masks. Results are shown in Table 6 and Fig. 6.

Method	Broom			Chicken			Peel-banana		
	mPSNR↑	mSSIM↑	mLPIPS↓	mPSNR↑	mSSIM↑	LPIPS↓	mPSNR↑	mSSIM↑	mLPIPS↓
TiNeuVox	19.633	0.609	0.659	24.103	0.777	0.264	21.558	0.863	0.267
TiNeuVox w/ Reg	20.955	0.774	0.628	26.006	0.949	0.196	22.313	0.891	0.274

Method	3dprinter			Tail			Toby sit		
	mPSNR↑	mSSIM↑	mLPIPS↓	mPSNR↑	mSSIM↑	mLPIPS↓	mPSNR↑	mSSIM↑	mLPIPS↓
TiNeuVox	19.184	0.780	0.296	22.593	0.822	0.511	18.191	0.783	0.611
TiNeuVox w/ Reg	19.323	0.775	0.318	23.191	0.891	0.438	19.385	0.790	0.536

Table 6: Evaluation of the proposed regularizer over the HyperNeRF vrig dataset.

Method	$d = 128$			$d = 256$			$d = 512$		
	mPSNR↑	mSSIM↑	mLPIPS↓	mPSNR↑	mSSIM↑	LPIPS↓	mPSNR↑	mSSIM↑	mLPIPS↓
TiNeuVox w/ Reg	15.441	0.609	0.415	15.981	0.618	0.401	16.221	0.671	0.399

Method	$d = 1024$			$d = 2048$			$d = 4096$		
	mPSNR↑	mSSIM↑	mLPIPS↓	mPSNR↑	mSSIM↑	mLPIPS↓	mPSNR↑	mSSIM↑	mLPIPS↓
TiNeuVox w/ Reg	17.254	0.677	0.381	17.887	0.712	0.367	18.036	0.777	0.361

Table 7: Ablation over the number of samples used for OT distance computation. Metrics are calculated over the iPhone dataset. As the number of samples grow, the performance improves, possible due to the lower error in OT computation as predicted by Theorem 1.

### A.3 FAILURE CASES

Since our method relies on an approximate OT distance, there can be instances where a pixel averaging effect occurs, resulting in a subtle blur. Interestingly, this effect can potentially cause a slight decline in the quality of renderings, especially when the baseline model already performs exceptionally well in a given sequence. Additionally, if the baseline model fails to converge completely in a particular sequence, our regularization technique may not yield substantial improvements in the results. Fig. 7 shows some examples.

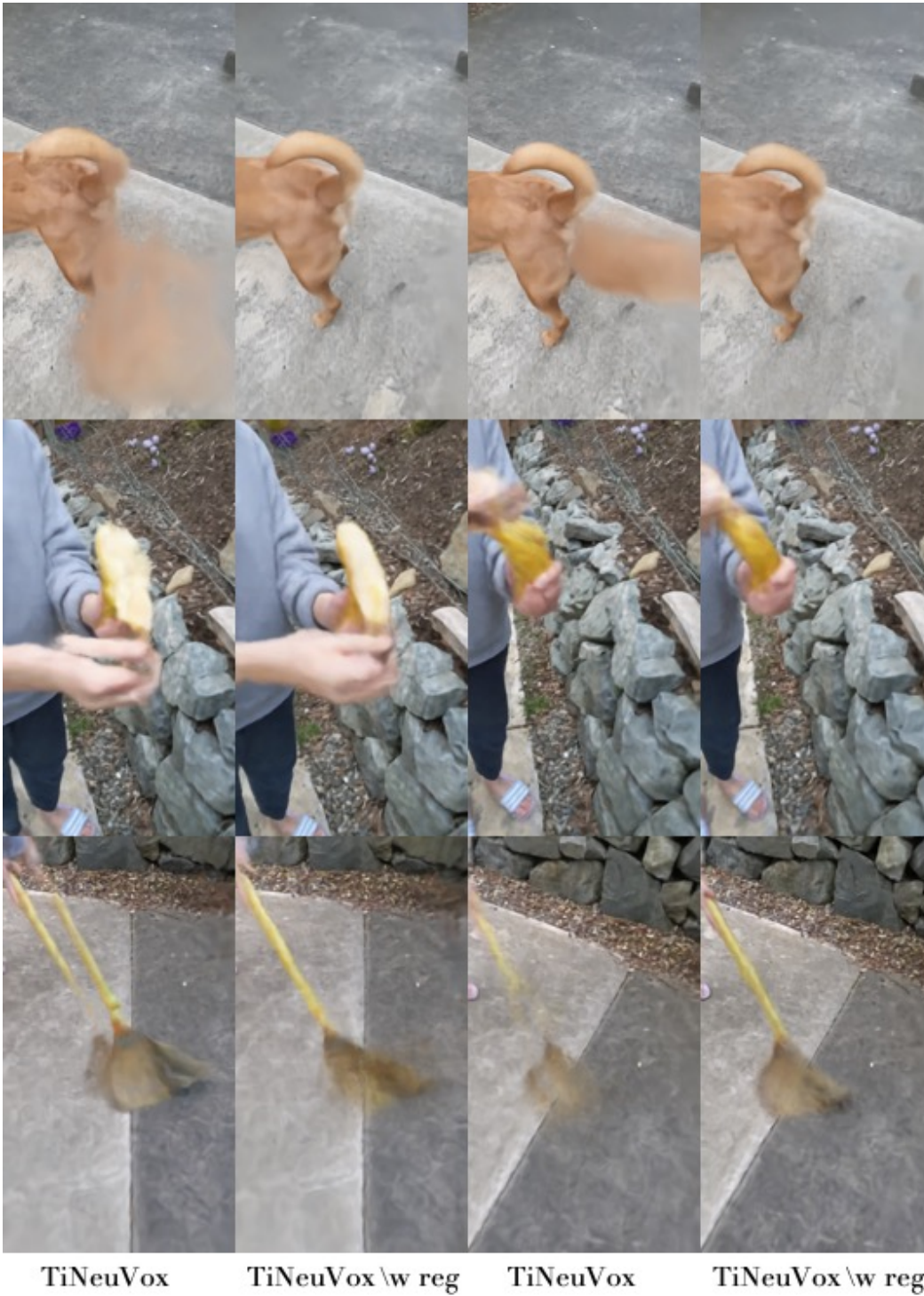


Figure 5: A qualitative illustration of the effect of the proposed regularization on the HyperNeRF vrig dataset.

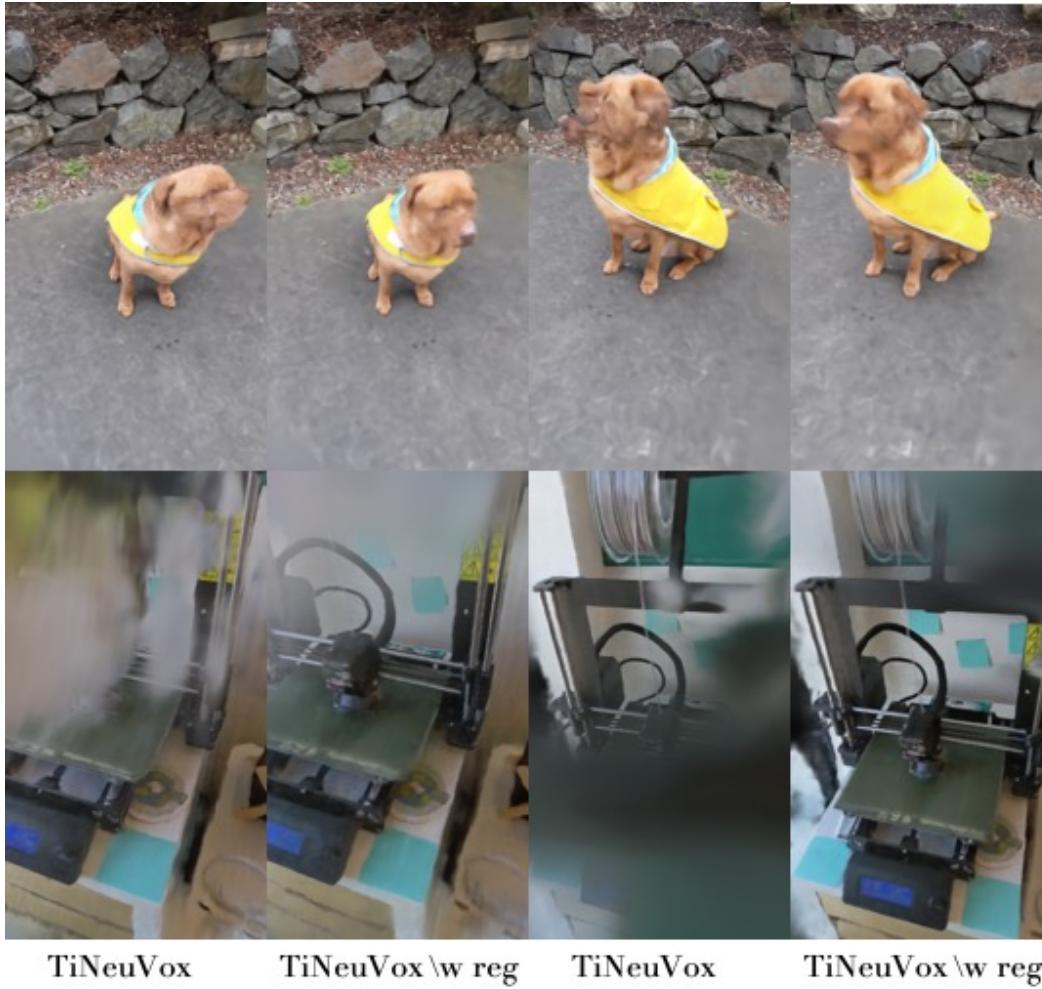


Figure 6: A qualitative illustration of the effect of the proposed regularization on the HyperNeRF vrig dataset.



Figure 7: **Example failure cases.** *Top row:* baseline, *bottom row:* baseline with regularization. Due to the pixel averaging effect that stems from the OT approximation sometimes degrade or does not improve the results. We observed cases where the baseline model performs too poorly, leading to our regularization not having much effect.